

Quantifying Resources for the Surmont Lease with 2-D Mapping and Multivariate Statistics

Weishan Ren, and Clayton V. Deutsch, University of Alberta,

David Garner, and T.J. Wheeler, ConocoPhillips Canada Ltd.,

Jean-François Richy, Emmanuel Mus, Total, seconded to ConocoPhillips Canada Ltd.

The McMurray formation consists of heterogeneous Cretaceous bitumen-saturated sands. The reservoirs are thick and laterally extensive in the main fairways. Many commercial projects are in the early stages of development. Resources too deep to mine are considering Steam Assisted Gravity Drainage (SAGD). Detailed high resolution 3-D geostatistical modeling is useful for individual well pair or pad flow simulation, but is neither practical nor necessary for resource assessment over large areas.

This paper presents a practical and tested methodology for resource assessment in the Surmont Lease. The uncertainty in over 30 correlated variables is calculated on a dense 2-D grid using all available information including wells, seismic and geologic trends. The correlation structure between the variables is modeled under a multivariate Gaussian model. The local distributions of uncertainty have been checked with cross validation and with more than 100 new wells drilled during the last two drilling seasons. Resource uncertainty over the entire lease area and a number of arbitrary development areas is derived from the 2-D maps of uncertainty. A combined P-field / LU simulation approach is used; the global uncertainty is consistent with the local uncertainty.

Introduction

The McMurray formation contains a large oil sands resource. A small portion of oil sands can be recovered by surface mining; most of bitumen resource will be produced by advanced heavy oil recovery technology such as the SAGD process. Accurate estimation of the in-situ resource range and associated risks is important for reservoir planning and development.

Detailed 3-D models of heterogeneity are useful. They provide numerical models consistent with small scale well data, measures of connectivity and visualizations that appear realistic. The challenge of 3-D models in the context of our problem is twofold: (1) the size of the models, and (2) the requirement for realistic summaries of reservoir quality at each location. The study area is more than 500 km², the thickness is on the order of 100m, there are more than 10 variables of interest and we would need 100 or more realizations to represent uncertainty. More than 20 billion numbers would need to be routinely manipulated to understand Surmont at a relatively coarse discretization of 50m x 50m x 1m.

The second challenge is more subtle. Reservoir management decisions depend in many factors such as the thickness of good quality reservoir, presence of top or bottom water, structure of the base reservoir and geological variability. These factors are, for the most part, areal summaries of the reservoir. They can be reliably calculated from the well data; however, they are not as reliably estimated from 3-D models. High resolution geostatistical models do not reproduce all of the complex geological features and trends. This challenge is addressed by research.

In summary, the advantages of using 2-D geostatistical modeling include (1) good estimates of reservoir quality consistent with available well data, (2) uncertainty at each location, (3) simple and fast modeling of variables required for decision making. This paper demonstrates the application of 2-D geostatistical modeling.

Several reservoir parameters are important. The thickness of net pay or net continuous bitumen thickness (NCB) is related to the height of an anticipated steam chamber. The bulk oil weight (BOW) measures the fraction of the bitumen mass to the total rock mass. The porosity (ϕ_{net}) and oil saturation (S_o) over the net continuous bitumen are related to the recoverable bitumen by the SAGD process. An important feature of many areas of the McMurray is the presence of top water and top gas that can provide a sink for the injected steam and adversely affect recovery. These upper units are referred to as thief zones for the injected steam. Each project and company identifies different critical parameters. The typical project will involve predicting 20 to 30 variables at each 2-D location. Only a few variables will be described in this review paper. Most of the data is derived from well logs and core data.

The available data variables are divided into two types: primary variables that we must predict and secondary variables that are established from geophysical interpretation or geological trend mapping. Secondary variables are used to constrain the prediction of primary variables away from the well data. The secondary variables are often structural variables. Three structural surfaces will be used in this paper: (1) the bottom surface of the McMurray formation (BSM), (2) the top surface of the McMurray formation (TSM), and (3) the Wabiskaw-McMurray surface (WMS), which is a maximum flooding surface above the McMurray formation. These structural data are usually quite reliable because of their lateral continuity and they are derived from a variety of data sources (well and seismic data). These three variables and the calculated gross thickness (GTM) of the McMurray are treated as independent secondary variables for the 2-D modeling.

Methodology: Local Uncertainty

Inference of uncertainty at unsampled locations requires the choice of a multivariate distribution. The multivariate distribution may be explicitly defined (the multivariate Gaussian distribution) or implicitly defined as in the cases of object based modeling or multiple point statistics. The latter implicit models are suited to a limited number of categorical variables. A multivariate Gaussian distribution is adopted in this paper. The methodology described below relates to implementation choices to infer the required parameters and process the resulting uncertainty.

All variables are transformed one-at-a-time into a standard normal or Gaussian distribution. A decision is then made that the joint distribution between all variables is multivariate Gaussian. This is a standard assumption. We check bivariate Gaussianity by displaying all cross plots – the probability contours should be elliptical with no non-linear, heteroscedastic or constraint features. The local distributions of uncertainty from the applied methodology are back transformed to original units. The multivariate Gaussian model has a long and established history in statistics and geostatistics. The specific implementation details used in this paper are described more fully in Deutsch and Zanon (2004).

The first step is to construct a conditional distribution of uncertainty in each variable at each location using the nearby well data. This is done with the normal equations, also known as simple kriging. These conditional distributions are defined by a mean and variance y_k^* and σ_k^2 . These distributions would be the final result if we had no secondary data. The presence of

secondary data must be considered. Following a loose Bayesian formalism we consider the following:

- Prior – local conditional distribution generated from surrounding well data of the same type,
- Likelihood – local conditional distribution generated from local data of different types, and
- Updated – local conditional distribution that accounts for the aforementioned distributions.

The likelihood distributions account for the secondary data that are available at every location. This is accomplished with the normal equations using the collocated N by N matrix of correlation coefficients. In our context, the matrix of correlation coefficients is symmetric, that is, $\rho_{ij}=\rho_{ji}$. The diagonal elements are all the variance of a standard Gaussian variable, which is 1. The correlation coefficients are calculated directly from the available data. The correlation coefficients between the secondary data are very well informed. The correlation coefficients between the primary and secondary data are calculated from values at well locations. These correlation coefficients are reasonably stable with more than 20 (or so) well data.

The matrix of correlation coefficients may not be positive definite if the values are calculated from different numbers of data. We often calculate the entire matrix from the observations at the well data locations, which ensures a positive definite result.

The conditional distribution due to the secondary data (the likelihood) is calculated from the correlation matrix and the secondary data. The likelihood distribution is defined by the mean y_L^* and variance σ_L^2 . These values summarize the information carried in all secondary data regarding the variable being predicted. There are different likelihood values for each primary variable being predicted. Consider n normal scores secondary data, $y_i, i=1, \dots, n$. The mean and variance are calculated as:

$$y_L^* = \sum_{i=1}^n \lambda_i \cdot y_i \quad (1)$$

$$\sigma_L^2 = 1 - \sum_{i=1}^n \lambda_i \cdot \rho_{i,0} \quad (2)$$

The weights $\lambda_j, j=1, \dots, n$ can be calculated by solving the n linear equations known as the normal equations and also known as simple kriging:

$$\sum_{j=1}^n \lambda_j \cdot \rho_{i,j} = \rho_{i,0} \quad i = 1, \dots, n \quad (3)$$

The two conditional distributions defined by (y_K^*, σ_K^2) and (y_L^*, σ_L^2) must be merged together to create an updated distribution. In the context of a multivariate Gaussian distribution and a Markov model of coregionalization, the updating of the prior distribution and the likelihood distribution is defined by:

$$y = \frac{y_L \sigma_K^{2*} + y_K \sigma_L^{2*}}{(1 - \sigma_L^{2*})(\sigma_K^{2*} - 1) + 1} \quad (4)$$

$$\sigma^2 = \frac{\sigma_K^{2*} \sigma_L^{2*}}{(1 - \sigma_L^{2*})(\sigma_K^{2*} - 1) + 1} \quad (5)$$

The location-dependent updated (y , σ^2) quantify the uncertainty at each location. The non-standard Gaussian distributions can be back transformed to original units to provide uncertainty in units that matter to us. The back transformation is non-linear, so the mean cannot be back transformed directly. Quantiles can be back transformed with no bias; therefore, the back transform of the final distribution requires transforming a large number of quantiles. The mean and variance in real units can be calculated using these transformed quantiles. The Gaussian mean and variance are kept because joint uncertainty requires simulation from them.

The three-step procedure of establishing the local conditional distributions is efficient. The three steps are (1) calculate the prior distribution, (2) calculate the likelihood distribution, and (3) merge the prior and likelihood distributions. There is an implicit Markov assumption in this approach, that is, the hard data perfectly screen the secondary data at the same location. Cross validation and checking with new drilling backs up this assumption; it is realistic.

The alternative multivariate Gaussian approach would be to fit a linear model of coregionalization to all variables and perform cokriging. This was considered impractical in the past; however, it would be possible with automatic variogram fitting and many well data. The advantage of the three step procedure is transparency and an easy way to understand the contributions of local well data and secondary data.

Methodology: Joint Uncertainty

The local uncertainty at small scale is represented by distributions of uncertainty in all of the primary variables. The primary variables are used to calculate the OOIP and categorize the reservoir by economic viability and/or thief zone type. The steps described above permit the calculation of uncertainty in each variable; however, there are two aspects of joint uncertainty that require simulation.

Firstly, the uncertainty in derived variables is a form of joint uncertainty. Consider the OOIP calculated as:

$$\text{OOIP} = 6.29 \times 10^4 \cdot \text{NCB} \cdot \phi_{\text{net}} \cdot \text{So}$$

Where the net continuous bitumen thickness, porosity, and bitumen saturation all enter into the calculation of OOIP. 6.29 is converts to barrels. In general, combining multiple correlated variables requires simulation.

Secondly, there is interest in the uncertainty in the bitumen resource over large areas such as a lease boundary or pad location. Local uncertainty, as described above cannot be simply combined to obtain the joint uncertainty over larger areas or scales.

The common feature of these two aspects is the presence of multiple variables and correlation. In the first multivariate case, there are relatively few variables (3 to 30) and the LU simulation approach is applicable. In the second multivariate spatial case, we choose a different simulation technique because of computer limitations. A sequential approach would work, but that would

require recalculating all of the conditional distributions in a random path using previously simulated values. It is desirable to draw all of the values simultaneously so that the large scale uncertainty is perfectly consistent with the local distributions of uncertainty. A multivariate Gaussian P-field-like simulation technique is used for spatial simulation.

Accounting for the correlation between multiple variables at the same location (NCB, ϕ_{net} , and So) is done with LU simulation. LU simulation has been used for many years, but popularized in geostatistics by Alabert, 1987. Multiple realizations (say 100) of the three variables are drawn accounting for the correlation between the variables (see yellow shaded squares in the table below). Then, the OOIP is calculated with each set of numbers. The uncertainty in the OOIP (or any other derived property) can be assembled from the realizations. A schematic table is shown below. Each set of three numbers (in yellow) is drawn by LU simulation using, for example, the LUSIM program from GSLIB (Deutsch and Journel, 1998).

Realization Number	NCB	ϕ_{net}	So	Calculated OOIP
1	10	0.30	0.85	160000 bbl
2	9	0.28	0.82	130000 bbl
...
100	11	0.27	0.83	155000 bbl

The LU method is suitable when the problem is small. The use of the LU method to simulate multiple dependent variables is straightforward. The matrix of correlation coefficients is decomposed by Cholesky decomposition: $C=LU$. A vector of uncorrelated standard normal values w is generated by a random number generator, then the correlated values are calculated by:

$$y_s = \mathbf{L} \cdot w \quad (6)$$

The y_s values have the right correlation structure, but they are standard Gaussian. The local conditional distributions of each variable are non-standard (see Equation 5); therefore, we account for that by non-standardizing the variables:

$$y_{ns} = y_s \bullet \sigma + y \quad (7)$$

The simulated realizations of non-standard values can be back transformed to original units and calculations performed, see table above.

The LU formalism described above can be performed at each location leading to uncertainty in derived variables at each location; however, there is often interest in uncertainty over multiple locations, perhaps the entire lease. To accomplish this joint simulation we use a P-field-like simulation technique. Unconditional standard normal variables are simulated for each of the n primary variables under consideration. The appropriate normal scores variogram used in the kriging of the prior distributions is used. The vector of unconditional simulated values at each location is taken as the w vector in Equation 6. The multiplication by L ensures that the values have the correct spatial correlation structure. Non-standardizing by Equation 7 ensures that all local information is accounted for. Then, the back transformed realizations can be processed for uncertainty calculations.

This procedure has many nice features. Firstly, it is easily performed with virtually all

geostatistical software packages. Secondly, it provides realizations of joint uncertainty that are perfectly consistent with the local uncertainty quantified above. Finally, it approximately reproduces the correct spatial structure as quantified by the input variograms and correlation matrix. There is a slight non-stationarity in the variogram structure of the simulated values: the continuity near conditioning data is slightly overstated. This is a well known feature of p-field simulation (Srivastava, 1992). Uncertainty in any arbitrarily large area is easily assembled from the multiple correlated realizations.

This provides a reasonable assessment of joint uncertainty; however, uncertainty in the input parameters is not considered in this analysis. A technique such as the spatial bootstrap could be used to assess uncertainty in the input parameters.

Resource assessment in the Surmont Lease

The Surmont Lease location and well data are given in Figure 1. A small area of the Surmont Lease is considered below.

2-D mapping

Five types of maps are generated for each reservoir parameter. The *trend* map is used to reveal the large scale trend in each parameter. The *prior* map is the kriging map of each parameter after being transformed to a Gaussian variable. These two maps are created for understanding each parameter independently. A correlation matrix plots the correlation between the variables. Based on the correlations, the *likelihood* map is created with the secondary data. The correlation matrix and the likelihood map provide information for understanding the correlation between the variables. Then, the Bayesian updating approach is applied to merge the prior models and likelihood models. This approach is similar to collocated cokriging, and is implemented in Gaussian space. The updated model contains the information from well data and from secondary data. The *updated* map shows the results of Bayesian updating in the Gaussian space. The updated Gaussian distributions must be back transformed to real units and are often summarized by the *final* maps, which are the $P_{10}/P_{50}/P_{90}$ maps of each parameter or the probability maps of these reservoir quality parameters at certain threshold.

Trend Maps

The trend map is used to provide the overall trend of each variable in the entire study area. This map is created by simple kriging with a variogram designed to reveal large scale features. Usually, a long range variogram (1/3 of the domain size) with modest nugget effect (30%) is used. All reservoir parameters are mapped with this trend variogram. As an example, the trend maps of the NCB and BOW are shown in Figure 2. Some high value zones are shown in the left of the study area for NCB.

Prior Maps

The prior model is also created by kriging but with the data in Gaussian space and the variogram calculated and fit from the well data. Variogram maps are helpful to find the direction of continuity in each parameter. Then, the directional variograms are calculated. The experimental variograms are modeled using a semi-automatic variogram fitting algorithm. The variogram and the model of the NCB are shown in Figure 3.

Kriging was then performed using these variogram models and the normal score data. The prior model generates an uncertainty distribution at each location. The uncertainty is a nonstandard

normal distribution with kriged mean and variance. The prior map for the NCB and BOW are also shown in Figure 2. They look similar to their trend maps but have more detailed small scale features. The values on these maps are only conditional to surrounding data of the same type; we still must consider the secondary data. If the prior maps do not show the large scale trend features from the trend maps, then kriging with a local mean is considered to impose the large scale trend values.

Correlation Matrix and Likelihood Maps

The cross plot of each pair of the variables is plotted to check the data and determine the correlation between each the pair of variables. Data that fall outside of a trend with the other data should be reviewed and perhaps eliminated to obtain a more representative correlation between the variables. Particular attention is paid to the three characteristic non-Gaussian features of (1) non linear relationship, (2) heteroscedastic variability, that is, changing variability of one variable as another variable changes, and (3) constraint features where one variable is constrained by other. The correlation coefficients are summarized and shown in a correlation matrix (Figure 4).

With the secondary data and the correlations between a primary reservoir variable and the secondary variables, we can calculate the likelihood for each reservoir variable. The four variables used for the secondary data are shown in Figure 5. The likelihood model provides a conditional distribution of each variable at each location conditional to collocated data of other types. The likelihood results are mapped to show the information from the secondary data. The likelihood maps of NCB and BOW are shown in Figure 6.

Updated Maps and Final Maps

Bayesian updating is used to merge the prior models and likelihood models. The resulting model is called the updated model. The uncertainty of each parameter at each location is generated from the information of well data and the secondary data. The uncertainty distribution is also a nonstandard normal distribution with updated mean and variance. The updated map shows the updated means in Gaussian space. The updated maps of NCB and BOW are shown in Figure 6.

The updated distribution needs to be transformed to real units to show the best estimate and the uncertainty at each location in real values. Usually, these features are summarized by P_{10} , P_{50} and P_{90} values. The P_{50} values provide estimates of each reservoir parameter at each location. We also consider the P_{10} and P_{90} values at those locations. The P_{10} low values provide a conservative estimate because there is a 90% probability of being larger than this value. The P_{10} map can also be used to identify the high value areas because when the P_{10} value is high then the value is surely high. The P_{90} values provide an optimistic estimate because there is a 90% probability of being less than this value. The P_{90} map can be used to identify the low valued areas because when the P_{90} value is low then the value is surely low.

All variables are predicted. The maps of local P_{10} , P_{50} and P_{90} values for NCB are shown in Figure 7. The green color in the P_{10} map shows where there is a 90% chance to have more than 25 meters of net continuous bitumen. The blue color in the P_{90} map shows where there is a 90% chance to be less than 20 meters of net continuous bitumen.

Validation

Reservoir modeling consists of many interdependent modeling steps with ample opportunity for mistakes and/or undue influence of problem data. It is impossible to completely validate models; however, there are some basic checks that can be used to identify problem data or errors in the geostatistical modeling. Cross validation is used to estimate the variables at locations where we

know the true value. The actual data are deleted one at a time and re-estimated from the remaining neighboring wells. Then, we can check the accuracy of the predicted distributions of uncertainty to evaluate the goodness of modeling parameters.

All well locations were used for cross validation. Likelihood calculations and updating were performed. Cross validation was performed with the Gaussian transforms of the original variables. The results were back transformed to original units.

Figure 8 shows the accuracy plots of the NCB and BOW. The width of symmetric probability intervals is plotted on the abscissa axis. The fraction of true values within the interval is plotted on the ordinate axis. In the accuracy plot, the points on the 45° line means that the model is both accurate and precise. If the points fall above the line, the model is accurate but not precise. If the points fall below the line, the model is neither accurate nor precise. Figure 8 shows that the model for NCB is accurate and precise.

A number of wells were drilled after these models were constructed. The goodness of the probabilistic estimates can be checked and compared to the new drilled wells. The results are shown in Figure 9. The model for NCB worked out extremely well.

The fairness of the probability values, that is, a good accuracy plot is not enough for good probabilistic predictions. The width or variance of the local distributions must also be narrow for good distributions.

Global resources assessment

There was an interest in the recoverable bitumen resource by SAGD and the original oil in place for SAGD (SAGD OOIP) in the Surmont lease and other arbitrarily large areas. We refer to these large areas as “global” to distinguish them from the “local” small 100m by 100m areas calculated in the 2-D models. The global SAGD OOIP was mostly affected by the net continuous bitumen thickness (NCB) and the presence of steam thief zones. A threshold of NCB=18m was considered as the minimum thickness for the economic recovery of bitumen with the current SAGD technology. When the presence of a certain thief zone is present, a minimum of 30m NCB is considered for SAGD to be economically successful. A lower 10m NCB cutoff was also considered to include the resource that could be used for future development when more advanced bitumen recovery technology becomes available. The global SAGD OOIP was calculated with different NCB cutoffs and for different thief zone types.

The calculation of SAGD OOIP and thief zone (TZ) type required six correlated variables: net continuous bitumen (NCB), net porosity (ϕ_{net}), net water saturation (S_w), thief zone protection factor (TZfactor), effective water thickness (EWT), and effective gas thickness (EGT). These variables had been analyzed as part of 2-D geostatistical studies.

$$\text{SAGD OOIP} = \text{NCB} \cdot \phi_{net} \cdot (1 - S_w)$$

$$\begin{aligned} \text{TZ type} &= 1, \text{ if TZfactor} \geq 5 \text{ m or (EWT} = 0 \text{ m and EGT} = 0 \text{ m)} \\ &= 2, \text{ if } (0.8 \text{ m} > \text{EWT} > 0\text{m}) \text{ or (EWT} = 0 \text{ m and EGT} > 0 \text{ m)} \\ &= 3, \text{ if EWT} \geq 0.8 \text{ m} \end{aligned}$$

The SAGD OOIP variable must be multiplied by area to get a volume. The uncertainty in global SAGD OOIP was a concern to the Surmont Team. It was calculated using the Bayesian updated 2-D models. An estimate of global SAGD OOIP from prior information alone was also

interesting. The logic and calculations used to assess uncertainty and to obtain the estimate over large regions of the Surmont lease are summarized as follows.

Uncertainty in Global SAGD OOIP

Uncertainty of small 100 m by 100 m areas or the incrementally larger LSD areas are captured very well by the 2-D models. Assessing uncertainty over larger scales, however, requires a different approach. Calculation of uncertainty from a local uncertainty measure to a regional or global uncertainty measure requires consideration of the spatial correlation within the region/domain because the assumption of independence between the smaller scale areas will drastically understate uncertainty at a large scale. The methodology presented above (also summarized in Ren et al., 2005) was used. The key steps are (1) construct local distributions of uncertainty (done already); (2) generate spatially correlated probability values; (3) draw values for all variables at all locations and keep them together as a realization. Step 1 has been done with priors, likelihoods and Bayesian updating with a multiGaussian kriging approach. Step 2 will use sequential Gaussian simulation. Step 3 will use LU simulation.

The reporting of uncertainty for an arbitrary volume required six proportions (in turquoise color in the table below): the proportion/probability of each of the three thief zone types and the proportion/probability of being above 10, 18, and 30 m NCB. Each of the six proportions was characterized by a distribution of uncertainty. Uncertainty was summarized by three values: a P_{10} , P_{50} , and P_{90} . These were shown in the turquoise boxes in the table below. Further, there was the distribution of uncertainty in the SAGD OOIP with no constraint on the thief zone type and no constraint on the net continuous bitumen (the bright yellow color square in the table below). There were six distributions of SAGD OOIP uncertainty for the three different thief zone types (no constraint on net continuous bitumen) and the three different NCB cutoffs (no constraint on thief zone type), which are shown in the pale yellow squares in the table below.

There were nine distributions of uncertainty in the SAGD OOIP for all combinations of the three thief zone types and the three NCB cutoffs (shown in the tan color in the table below). These distributions of uncertainty had P_{10} , P_{50} , and P_{90} values for SAGD OOIP, as well as P_{10} , P_{50} , and P_{90} values for the proportion of values within the NCB/TZ class (shown in turquoise boxes above the tan boxes below).

Uncertainty for an Arbitrary Volume			Thief Zone Type			
			No Constraint	TZ1	TZ2	TZ3
				$P_{10} / P_{50} / P_{90}$	$P_{10} / P_{50} / P_{90}$	$P_{10} / P_{50} / P_{90}$
NCB Cutoff	No Constraint	$P_{10} / P_{50} / P_{90}$				
	NCB > 10	$P_{10} / P_{50} / P_{90}$				
	NCB > 18	$P_{10} / P_{50} / P_{90}$				
	NCB > 30	$P_{10} / P_{50} / P_{90}$				

In summary, 3+3+9=15 distributions of proportions (three numbers each) and 1+3+3+3•3=16 distributions of SAGD OOIP uncertainty (three numbers each) were used to report the uncertainty for an arbitrary volume: 93 numbers in all. Uncertainty was tabulated according to the format shown above.

The underlying models of uncertainty were created at a 100 m by 100 m areal scale. Uncertainty

at this scale is dominated by the spacing of nearby wells and the available secondary data variables. This uncertainty can be straightforwardly scaled up to the LSD scale (about 400 m by 400 m) by arithmetic averaging under an assumption that the values are highly correlated over a 400 m scale.

The uncertainty at the 100 m or LSD scale was represented by distributions of uncertainty in all of the variables including net continuous bitumen (NCB), net porosity (ϕ_{net}), net water saturation (S_w), thief zone protection factor (TZfactor), effective water thickness (EWT), and effective gas thickness (EGT). The uncertainty in each of these variables does not give uncertainty in SAGD OOIP or TZ type. The correlation between these variables and the spatial correlation within the region/domain must be taken into account.

Accounting for the correlation between NCB, ϕ_{net} , ..., and EGT was done with simulation. Multiple realizations ($L=100$) of the six variables were drawn accounting for the correlation between the variables and the spatial correlation within the region/domain (see purple shaded squares in the table below). Then, with each set of six numbers the SAGD OOIP and TZ type were calculated (see yellow squares on the right). The results were analyzed to fill in the uncertainty table.

Real #	NCB	ϕ_{net}	S_w	TZPF	EWT	EGT	SAGD OOIP	TZ Type
1								
2								
3								
...								
L								

There are a number of simulation techniques in use throughout statistics and geostatistics. The LU method (named after the Cholesky LU matrix decomposition method) has been around for a long time and is suitable when the problem is small. For example, consider assessing uncertainty in the SAGD OOIP and TZ type at a particular location, that is, filling in a table as shown above.

The use of the LU method to simulate multiple dependent variables is straightforward. Only the correlation matrix between the six variables was required, and a set of correlated normal scores was required to account for the spatial correlation of the variables. The latter requirement was satisfied by generating unconditional realizations using sequential Gaussian simulation for each of the six variables.

The simulated variables were then used to calculate the corresponding SAGD OOIP and TZ type at each location. This was performed for multiple realizations and the uncertainty was assessed. The resulting distributions of uncertainty are shown in Table 1.

Uncertainty depends on the amount of local well data, the secondary data variables and the modeling approach and parameters. We have observed a consistent decrease in uncertainty as additional delineation wells are drilled.

Conclusion

A 2-D geostatistical modeling process is demonstrated to characterize the reservoir quality of the McMurray formation. Many different maps were created to reveal different aspects of the reservoir properties and their uncertainty. Trend maps and prior maps can be used to understand the variability of the reservoir parameter independent of any secondary information. The likelihood maps can be used to show the information from the secondary data. The updated maps contain the information from the well data as well as from the secondary data. The local uncertainty is accessed by the 2-D models, and the P10, P50, and P90 maps provide heterogeneity and uncertainty information on the bitumen reservoir properties. Moreover, the global uncertainty is assessed by post process methods.

There are limitations to the approach. Detailed 3-D models of heterogeneity must be constructed separately. There is a strong reliance on stationarity and multivariate Gaussianity; subdividing the area or considering local changes in modeling parameters may be required. The sources of uncertainty (sensitivity) must be understood separately.

Despite these limitations, the 2-D mapping methodology has great applicability for resource assessment. Multiple data types are integrated accounting for their information content and a defensible model of uncertainty is generated.

Acknowledgements

The authors would like to thank the Surmont Team including ConocoPhillips and Total for permission to publish this paper.

References

- Alabert, F. G. 1987, The practice of fast conditional simulations through the LU decomposition of the covariance matrix, *Mathematical Geology*, 19(5), p. 369-386.
- Deutsch, C. V. and Journel, A. G., 1998, *GSLIB: Geostatistical Software Library and User's Guide*, Oxford University Press, New York.
- Deutsch, C. V. and Zanon, S., 2004, Direct Prediction of Reservoir Performance with Bayesian Updating Under a Multivariate Gaussian Model, Paper presented at the Petroleum Society's 5th Canadian International Petroleum Conference (55th Annual Technical Meeting), Calgary, Alberta.
- McLennan, J. and Deutsch, C.V., 2003, Guide to SAGD Reservoir Characterization Using Geostatistics, Center for Computational Geostatistics, University of Alberta, Edmonton, Alberta.
- Ren, W., Leuangthong, O., and Deutsch, C. V., 2005, Global Resource Uncertainty Using a Spatial/Multivariate Decomposition Approach, Paper presented at the Petroleum Society's 6th Canadian International Petroleum Conference (56th Annual Technical Meeting), Calgary, Alberta.
- Srivastava, R. M., 1992, Reservoir characterization with probability field simulation, *SPE Formation Evaluation*, 7(4), p. 927-937.

Nomenclature

- n = number of data used in a calculation
 y = normal score transform of a variable
 σ = standard deviation
 λ = weight calculated by normal equations
 ρ = correlation coefficient

Subscripts

- K = prior distribution from same data type
 L = likelihood distribution from same secondary
 s, ns = standard Gaussian, non-standard Gaussian
 i, j = data indices
 o = index for location being estimated

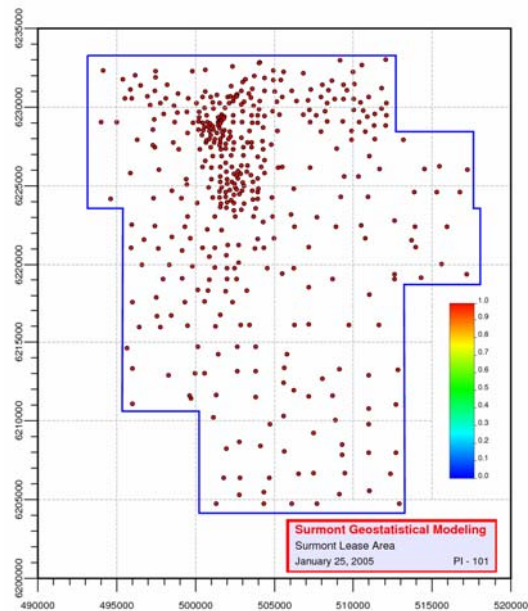


Figure 1: The Surrmont lease map with well locations.

Sw	-0.09	-0.13	-0.15	0.04	-0.03	-0.51	-0.23	1.00
Phi	0.10	0.20	0.21	0.00	0.26	0.87	1.00	-0.23
BOW	0.18	0.27	0.29	-0.06	0.32	1.00	0.87	-0.51
NCB	-0.04	0.41	0.43	0.29	1.00	0.32	0.26	-0.03
GTM	-0.86	-0.09	-0.08	1.00	0.29	-0.06	0.00	0.04
WMS	0.55	0.97	1.00	-0.08	0.43	0.29	0.21	-0.15
TSM	0.56	1.00	0.97	-0.09	0.41	0.27	0.20	-0.13
BSM	1.00	0.56	0.55	-0.86	-0.04	0.18	0.10	-0.09
	BSM	TSM	WMS	GTM	NCB	BOW	Phi	Sw

Figure 4: The correlation matrix of the 11 variables

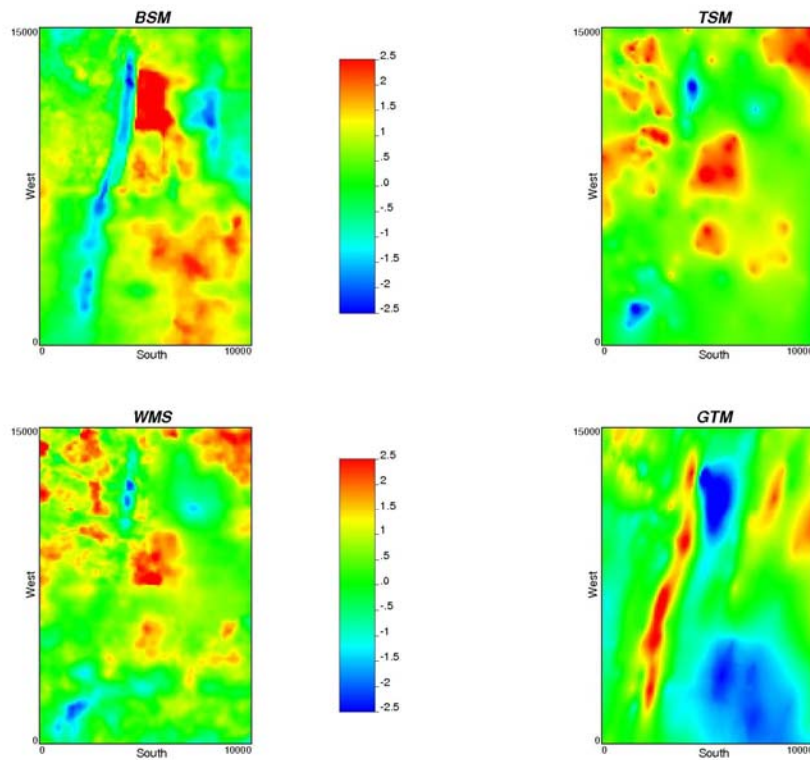


Figure 5: The maps of the four secondary data

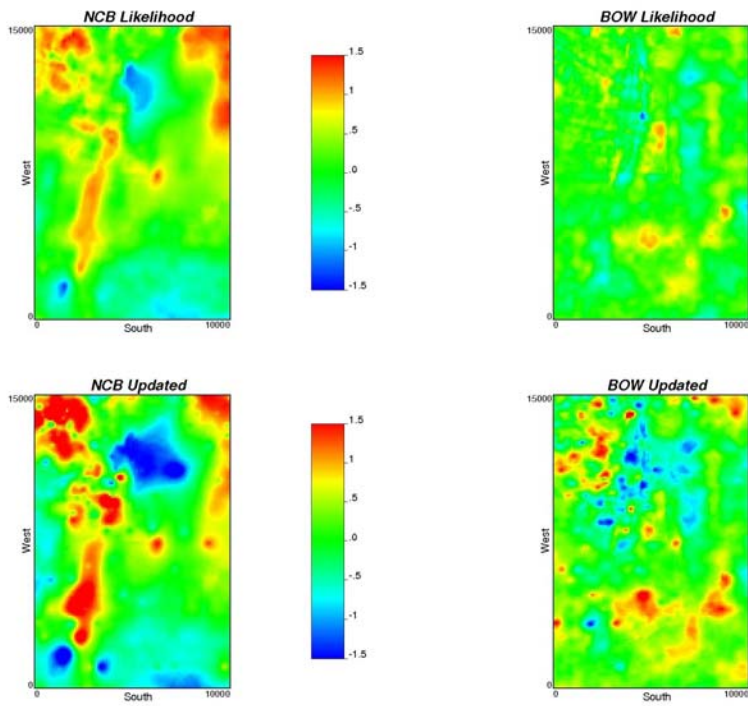


Figure 6: The likelihood maps (top) and the updated maps (bottom) of NCB and BOW.

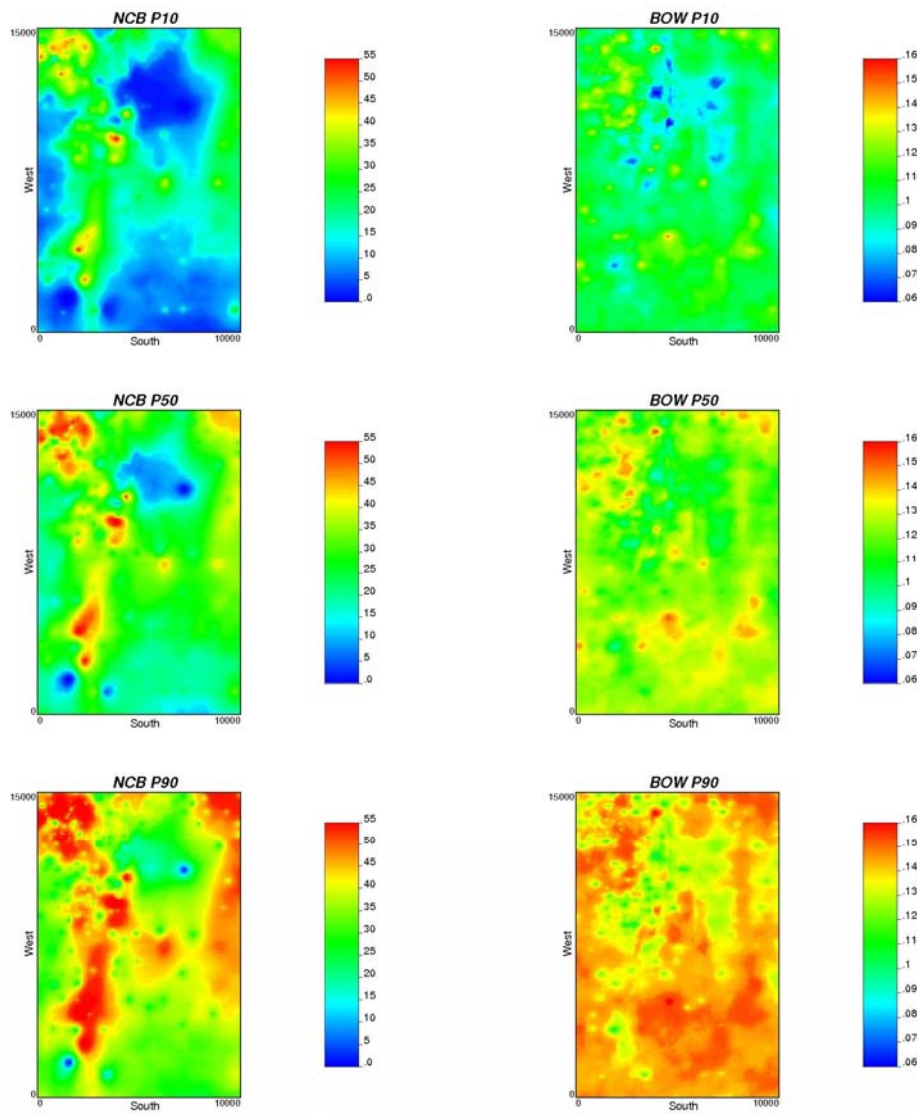


Figure 7: Maps summarizing uncertainty in NCB (left) and BOW (right). The P10 low values are shown at the top, the P50 values are shown in the middle and the P90 high values are shown at the bottom.

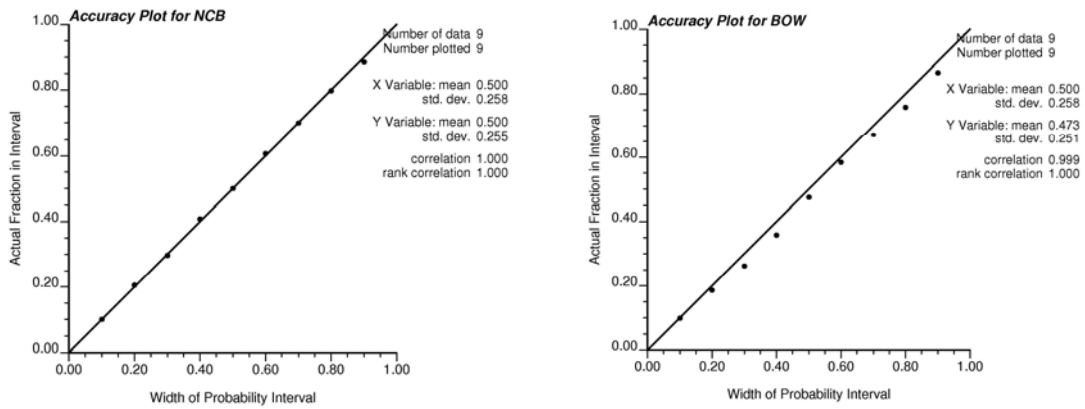


Figure 8: The accuracy plots of cross validation results for NCB and BOW.

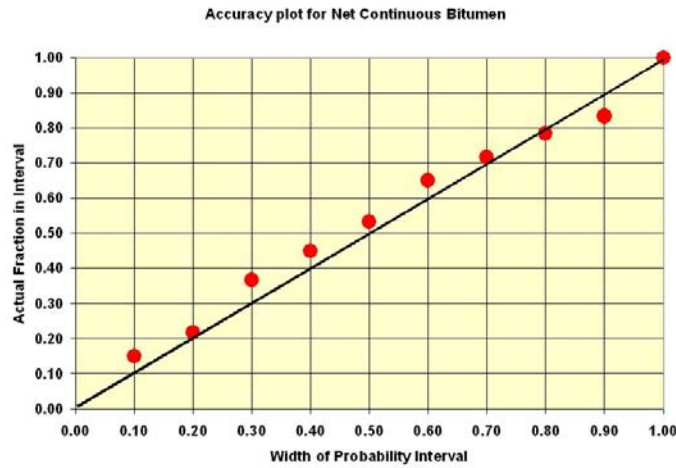


Figure 9: Accuracy plot of 2-D model vs. new wells of 2004

Uncertainty for Lease Area		Thief Zone Type			
		No Constraint	TZ1	TZ2	TZ3
NCB Cutoff	No Constraint	0.864 / 1.000 / 1.156	0.392 / 0.418 / 0.445	0.214 / 0.228 / 0.243	0.329 / 0.353 / 0.382
	NCB > 10	0.652 / 0.715 / 0.784	0.238 / 0.258 / 0.282	0.110 / 0.127 / 0.150	0.295 / 0.328 / 0.361
	NCB > 18	0.535 / 0.602 / 0.689	0.196 / 0.219 / 0.249	0.069 / 0.082 / 0.103	0.263 / 0.300 / 0.338
	NCB > 30	0.294 / 0.365 / 0.446	0.119 / 0.142 / 0.172	0.014 / 0.020 / 0.030	0.163 / 0.200 / 0.246
			0.324 / 0.371 / 0.429	0.099 / 0.118 / 0.141	0.408 / 0.475 / 0.566
			0.299 / 0.348 / 0.410	0.075 / 0.091 / 0.116	0.389 / 0.459 / 0.551
			0.219 / 0.271 / 0.333	0.021 / 0.030 / 0.045	0.284 / 0.357 / 0.455

Total No. Blocks = 55483

Table 1: The Surmont Lease resource estimation and uncertainty assessment: the blue shaded boxes are proportions and the others are barrels – standardized to “1.000” for the lease.